

Light induced excited high spin-state trapping in $[\text{FeL}_2](\text{BF}_4)_2$ ($\text{L} = 2,6\text{-di}(\text{pyrazol-1-yl})\text{pyridine}$)

Victoria A. Money,^a Ivana Radosavljevic Evans,^a Malcolm A. Halcrow,^b Andrés E. Goeta^a and Judith A. K. Howard^{*a}

^a Chemistry Department, Durham University, South Road, Durham, UK DH1 3LE.

E-mail: j.a.k.howard@durham.ac.uk

^b Department of Chemistry, University of Leeds, Leeds, UK LS2 9IT

Received (in Cambridge, UK) 16th October 2002, Accepted 22nd November 2002

First published as an Advance Article on the web 5th December 2002

The spin-crossover complex $[\text{FeL}_2](\text{BF}_4)_2$ undergoes a LIESST transition at 30 K on irradiation; the structures of the low-spin ground and high-spin metastable states at this temperature are presented.

The first iron(II) spin-crossover compound was reported by Baker and Bobonich in 1964.¹ Since then there has been much interest in these materials due to their potential for applications such as information storage, molecular switches and visual displays.² In the mid 1980s Decurtins *et al.* reported the first case of a transition from low to high spin caused by irradiation, the LIESST effect (Light Induced Excited High Spin-State Trapping).³ This opened up the possibility of these materials being used in optical devices. The metastable high-spin states, HS-2, formed in this way have been found to have very long lifetimes at low temperatures with the highest reported LIESST temperature, as defined by Létard *et al.*,⁴ being 130 K.⁵ Crystallographic structures of the HS-2 state have been reported in only a small number of cases, two recent examples being the studies by Kusz *et al.* in 2001⁶ and Marchivie *et al.* in 2002.⁷

In comparison with many spin-crossover compounds in which the transition is very gradual and the low-spin state, LS, is only stable at very low temperatures, $[\text{FeL}_2](\text{BF}_4)_2$ (Fig. 1)† shows an abrupt thermal spin transition centred at 260 K with a small hysteresis loop of 3 K.⁸ The relatively high temperature of the transition combined with the molecular bistability indicated by the hysteresis makes this compound very interesting for the applications mentioned above. We have therefore undertaken a further X-ray diffraction study of this system in order to probe the changes in its molecular and crystal structure over a wide temperature range.

Single crystal X-ray diffraction data† were collected at 290(2), 120(2), 30(2) K and after irradiation at 30(2) K. The structures of the high-spin state at 290(2) K, HS-1, and 120(2) K, LS, show good agreement with the published data.⁸ On flash freezing to 30(2) K the crystal remains in the monoclinic space group $P2_1$. Unlike the isomeric spin crossover compound $[\text{Fe}(\text{bpp})_2](\text{BF}_4)_2$ ($\text{bpp} = 2,6\text{-bis}(\text{pyrazol-3-yl})\text{pyridine}$),⁹ $[\text{FeL}_2](\text{BF}_4)_2$ is not trapped in a metastable state on flash freezing, most likely owing to the relatively high temperature of the thermal spin transition. Flash freezing of the sample was necessary due to degradation of the crystals on slow cooling, which it was thought might be due to a further phase change. However, the variation of the unit cell volume between 30 K and 260 K, accurately determined from variable temperature powder X-ray diffraction data (Fig. 2), shows an abrupt increase which corresponds to the transition to the HS-1 and eliminates the possibility of an additional phase change in this temperature range. From these data, a thermal expansion tensor was calculated and the obtained volume coefficient of thermal

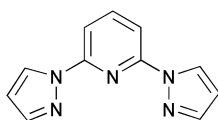


Fig. 1 $\text{L} = 2,6\text{-Di}(\text{pyrazol-1-yl})\text{pyridine}$.

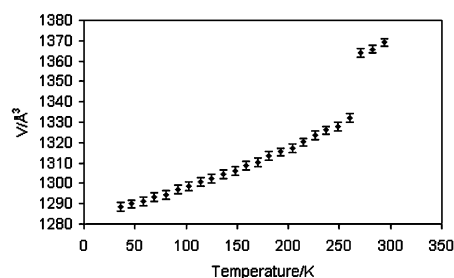


Fig. 2 Change in unit cell volume on warming from 30(2) to 300(2) K determined by variable temperature powder X-ray diffraction.

expansion at 50 K is $\alpha_V = 1.07 \times 10^{-4} \text{ K}^{-1}$. The spin transition is accompanied by a thermochromic effect in which the crystal changes colour from yellow in the high-spin state to brown in the low-spin state. Table 1 shows several key parameters which differ for each spin state.

The crystal was irradiated with a He–Ne laser ($\lambda = 632.8 \text{ nm}$, 15 mW) at 30(2) K for 30 min. It was noted that after irradiation the crystal had changed colour from brown to yellow implying that the HS-2 state had been formed. Data were collected on the irradiated crystal at 30(2) K. The Fe–N bonds have an average length of 2.165(2) Å, indicative of Fe(II) in the HS state. This increase in average ligand–metal bond length of 0.213 Å is comparable to reported results for spin transitions of Fe(II) bonded to six nitrogen donors.^{10,11} The volume of the unit cell

Table 1 Selected structural parameters at various temperatures

Spin state	T/K	$V/\text{Å}^3$	$\beta/^\circ$	Mean Fe–N/Å	Bite angle	BF_4^-
HS-1	290	1373.3(5)	95.67(3)	2.166(6)	73.4(2)	Disordered
LS	120	1308.6(5)	98.37(3)	1.953(2)	80.09(8)	Ordered
LS	30	1288.8(1)	98.575(1)	1.950(2)	80.08(8)	Ordered
HS-2	30	1318.1(5)	97.15(1)	2.165(2)	73.52(7)	Ordered

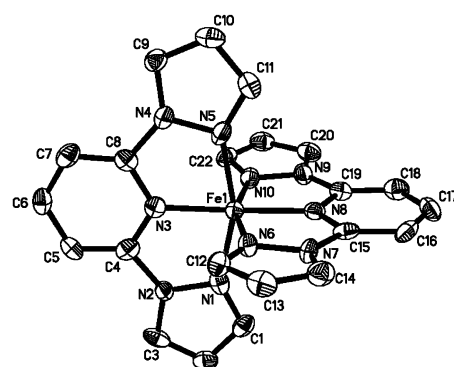


Fig. 3 Molecular structure of low-spin $[\text{FeL}_2]^{2+}$ at 30 K showing the numbering scheme used for the complex cation. Hydrogen atoms have been omitted for clarity. Thermal ellipsoids are at 90% probability.

was found to be $1318.1(5) \text{ \AA}^3$. This is an increase of 29.3 \AA^3 equal to 2.3% on going from the LS to the HS-2 state. This is in good agreement with the 2.6% increase calculated for the thermal spin transition⁸ and in the range expected for mononuclear Fe(II) materials.^{12,13} However the similarity between the increase in volume, ΔV_{SC} , in the thermal and light induced transitions is unusual. In the two cases mentioned above ΔV_{SC} has been found to be significantly less for the light induced transition than reported for the thermal transition.^{6,7} Crystalline $[\text{FeL}_2](\text{BF}_4)_2$ is very tightly packed with a non hydrogen atom volume of 15 \AA^3 and this may account for the similarity in the ΔV_{SC} values. Significant differences in the molecular geometry of the two spin states are not restricted to the ligand metal bonds. There is a shortening of all N–N bonds on going from the LS to the HS-2 state which is most pronounced in those rings forming the shortest Fe–N bonds. This decrease in bond length is probably due to an increase in t_{2g} back bonding in the HS-2 state; it is thought that the shorter metal ligand bonds in the LS state increase the degree of backbonding due to enhanced overlap between the orbitals. As a result of the change in Fe–N bond lengths the ligand bite angle is decreased from an average value of $80.08(8)^\circ$ for the LS complex to $73.52(7)^\circ$ for the HS-2 state. The N3–Fe1–N8 bond angle changes from $177.7(1)^\circ$ for the LS state to $169.68(8)^\circ$ for the HS-2 state. All the Fe–N bonds in the HS-2 structure at 30(2) K are within an esd of the equivalent bond lengths at room temperature. The structure of the HS-2 cation at 30(2) K is very similar to that determined at room temperature, however no disorder is found in the BF_4^- anions at 30(2) K.

Variation of the unit cell volume with temperature after irradiation shows an abrupt decrease from 1333(2) to 1302(7) \AA^3 , Fig. 4. The discontinuity coincides with the colour change of the crystal from yellow to brown. The LIESST transition, as determined by X-ray diffraction measurements, therefore takes place between 80(2) K and 85(2) K. The volume coefficient of thermal expansion of HS-2 at 50 K is $\alpha_v = 0.71 \times 10^{-4} \text{ K}^{-1}$. The changes in cell parameters during relaxation from HS-2 to LS show a pronounced anisotropy. The same trend is seen in the thermal transition between LS and HS-1. The change of the crystallographic c parameter is more than five times that in either a or b . This could be due to the Fe–N bonds to the central pyridine ring (Fe–N3 and Fe–N8), which lie in the direction of the c axis and show the largest change in length over the transition. It is possible that intermolecular bonding also plays a part: edge-to-face and face-to-face interactions lie along the a and b axis whilst there is some hydrogen bonding between CH and F atoms along the c axis.

Photomagnetic measurements are underway to confirm the exact temperature of the transition, the degree of conversion obtained by irradiation and to determine the effect of continued irradiation on the LIESST temperature. Planned infrared spectroscopy on the irradiated sample will enable us to determine the rate of relaxation from the HS-2 state to the ground LS state.

The authors would like to thank Dr A. Beeby for assistance with the LIESST experiments, Dr J. S. O. Evans for help with the powder diffraction experiments and the EPSRC for a

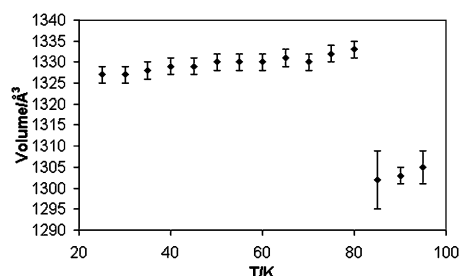


Fig. 4 Change in unit cell volume of a single crystal of $[\text{FeL}_2](\text{BF}_4)_2$ on warming after irradiation.

studentship (V. A. M.) and for a Senior Research Fellowship (J. A. K. H.).

Notes and references

† *Synthesis*: Crystals and polycrystalline powder of $[\text{FeL}_2](\text{BF}_4)_2$ were synthesised as described in the literature.⁸

Crystal data: $\text{C}_{22}\text{H}_{18}\text{N}_{10}\text{FeB}_2\text{F}_8$, $M_r = 651.93$, monoclinic, $P2_1$, $Z = 2$. **30(2) K**: $a = 8.4098(4) \text{ \AA}$, $b = 8.4731(4) \text{ \AA}$, $c = 18.2909(9) \text{ \AA}$, $\beta = 98.575(1)^\circ$, $V = 1288.8(1) \text{ \AA}^3$, $D_c = 1.680 \text{ Mg m}^{-3}$, $\mu = 0.679 \text{ mm}^{-1}$, $\lambda(\text{Mo-K}\alpha) = 0.71073 \text{ \AA}$. Selected crystal, $0.20 \times 0.18 \times 0.06 \text{ mm}$, mounted on a hair in fluoropolyether oil and flash frozen in a chilled helium gas flow at 30(2) K using an Oxford Cryosystems HELIX.¹⁴ 11476 reflections ($2.65 < \theta < 27.45^\circ$) collected on Bruker SMART-CCD diffractometer (ω -scan, $0.3^\circ/\text{frame}$) yielding 5434 unique data ($R_{\text{int}} = 0.0335$). The structure was solved by direct methods and refined by full matrix least squares based on F^2 for all data using SHELXL software. All non-hydrogen atoms were refined with anisotropic refinement factors, H-atoms were placed geometrically at calculated positions and refined with a riding model. Final $wR(F^2) = 0.0691$ and $R(F) = 0.0358$ for all data (388 refined parameters), GOF = 1.023, residuals $\Delta\rho_{\text{min,max}} = -0.447, 0.430 \text{ e \AA}^{-3}$. CCDC 195715. **30(2) K after irradiation**: $a = 8.461(2) \text{ \AA}$, $b = 8.370(2) \text{ \AA}$, $c = 18.759(4) \text{ \AA}$, $\beta = 97.15(3)^\circ$, $V = 1318.1(5) \text{ \AA}^3$, $D_c = 1.640 \text{ Mg m}^{-3}$, $\mu = 0.663 \text{ mm}^{-1}$, $\lambda(\text{Mo-K}\alpha) = 0.71073 \text{ \AA}$. Selected crystal mounted, $0.24 \times 0.20 \times 0.12 \text{ mm}$, and cooled to 30(2) K, data collected as above after irradiation for 30 min with an He–Ne laser ($\lambda = 632.8 \text{ nm}$, 15 mW). Structure solution and refinement methods as above. 11729 reflections collected ($R_{\text{int}} = 0.0281$), 5269 unique. Final $wR(F^2) = 0.0759$, $R(F) = 0.0310$ for all data (388 refined parameters), GOF = 1.058, residuals $\Delta\rho_{\text{min,max}} = -0.639, 0.582 \text{ e \AA}^{-3}$. CCDC 195714. See <http://www.rsc.org/suppdata/cc/b2/b210146g/> for crystallographic data in CIF or other electronic format. *Variable temperature powder X-ray diffraction*: data were collected using a Bruker AXS D8 Advance diffractometer equipped with an Oxford Cryosystems PHENIX helium cryostat¹⁵ and a Braun linear PSD. A total of 24 patterns were collected between 30 and 300 K, with a heating rate of 17 K h^{-1} , in the 2θ range between 5 and 35° in 0.0144° steps, using a counting time of 0.85 s/step , resulting in a collection time of 30 minutes per range. The model obtained from single crystal data was used to carry out Rietveld refinements of the 24 powder patterns. The only structural parameters refined were the cell parameters and an overall isotropic temperature factor. The other parameters refined were sample displacement, six background terms and six terms describing a pseudo Voigt profile function.

- W. A. Baker and H. M. Bobonich, *Inorg. Chem.*, 1964, **3**, 1184.
- P. Gütllich, A. Hauser and H. Spiering, *Angew. Chem. Int., Ed. Engl.*, 1994, **33**, 2024; P. Gütllich, Y. Garcia and H. A. Goodwin, *Chem. Soc. Rev.*, 2000, **29**, 419.
- S. Decurtins, P. Gütllich, K. M. Hasselbach, H. Spiering and A. Hauser, *Inorg. Chem.*, 1985, **24**, 2174.
- J.-F. Létard, L. Capes, G. Chastanet, N. Moliner, S. Létard, J.-A. Real and O. Kahn, *Chem. Phys. Lett.*, 1999, **313**, 115–120.
- S. Hayami, Z. Gu, Y. Einaga, Y. Kobayashi, Y. Ishikawa, Y. Yamada, A. Fujishima and O. Sato, *Inorg. Chem.*, 2001, **40**, 3240.
- J. Kusz, H. Spiering and P. Gütllich, *J. Appl. Crystallogr.*, 2001, **34**, 229.
- M. Marchivie, P. Guionneau, J. A. K. Howard, A. E. Goeta, G. Chastanet, J.-F. Létard and D. Chasseau, *J. Am. Chem. Soc.*, 2002, **124**, 194.
- J. M. Holland, J. A. McAllister, C. A. Kilner, M. Thornton-Pett, A. J. Bridgeman and M. A. Halcrow, *J. Chem. Soc., Dalton Trans.*, 2002, 548; J. M. Holland, J. A. McAllister, Z. Lu, C. A. Kilner, M. Thornton-Pett and M. A. Halcrow, *Chem. Commun.*, 2001, 577.
- S. Marcén, L. Lecren, L. Capes, H. A. Goodwin and J.-F. Létard, *Chem. Phys. Lett.*, 2002, **359**, 87–95.
- P. Guionneau, C. Brigouleix, Y. Barrans, A. E. Goeta, J.-F. Létard, J. A. K. Howard, J. Gaultier and D. Chasseau, *C. R. Acad. Sci., Ser. II: Chim.*, 2001, **4**, 161.
- E. König, *Prog. Inorg. Chem.*, 1987, **35**, 527.
- Y. Garcia, P. Guionneau, G. Bravic, D. Chasseau, J. A. K. Howard, O. Kahn, V. Ksefontov, S. Reiman and P. Gütllich, *Eur. J. Inorg. Chem.*, 2000, 1531.
- P. Guionneau, M. Marchivie, G. Bravic, J.-F. Létard and D. Chasseau, *J. Mater. Chem.*, 2002, **12**, 2546.
- A. E. Goeta, L. K. Thompson, C. L. Sheppard, S. S. Tandon, C. W. Lehmann, J. Cosier, C. Webster and J. A. K. Howard, *Acta Crystallogr., Sect. C*, 1999, **55**, 1243.
- Variable temperature powder diffraction studies made possible by EPSRC/JREI Grant number GR/M35222.